TECHNICAL PAPER

Investigation of static and fatigue behavior of honeycomb sandwich structure: a computational approach

Amit Amulani[1] · Hemant Pratap[1] · Benedict Thomas[1]

Abstract

Honeycomb Sandwich Composites are extensively used in high structural applications owing to their low weight and high stiffness properties. Various material combinations were investigated computationally to attain improved static and fatigue response. Aluminium 7075-T6 as honeycomb core and Ti-6Al-4V as face sheet was found to be the best combination. The fatigue response of the specimen was carried out as per ASTM C393 standard. Using the same, the static bending tests were also carried out. The proposed honeycomb structure was modeled and Finite Element Analysis was performed in ANSYS. There was a good agreement between theoretical and simulated results carried out for static deflection. The fatigue life of the specimen was validated with the results available in the literature. The reduction in fatigue life associated with load value was found out to be approximately linear. Further, experimental analysis was carried out to validate computational work. The obtained results presented exceptional fatigue behavior of the proposed honeycomb composite. The proposed material combination is expected to have great feasibility in aerospace applications based on the findings.

Keywords Honeycomb sandwich · Composite · Finite element analysis · Fatigue life · Static behavior

1 Introduction

With the advancement in the aircraft industry, the caliber and function of craft fabrication have proved to meet the bizarre demands and performances. These specifications have generally highlighted the structural designs as light-weight (including high specific strength, stiffness, and toughness). Therefore, researchers have studied the new aspect of multifunctional and lightweight materials to represent a conventional system with different functions and parameters, hence the concept of honeycomb sandwich rises. These composites have good structure, material, and functional design [1]. They have higher axial stiffness and are created to reduce the weight of the overall geometry to achieve high strength-to-weight, stiffness-to-weight ratios, and thermal resistance. At present, that materials which offer low density, long-term performance under different loading

conditions, high stiffness, and strength are preferred. Also, high bending stiffness is a key asset in developing models with multilayer materials. So, considering only static behavior of the specimen will be insufficient; therefore, understanding fatigue behavior is also very significant for the composites [2].

The use of honeycomb in various fields is indisputable. In engineering background, it has made the researchers explore by taking various experiments and designing the models. The sandwich composite mainly consists of three components. The core, which is made up of material having low density. The designed model carries out adequate shear strength to resist the transverse shear stresses, thick enough to withstand buckling, and provides high stiffness. The two face sheets separated by core, contains strong material to resist the high forces due to loading and should be relatively stiff. The two factors that are crucial to achieve high strength and stiffness are cell geometry and material [3].

The static behavior of honeycomb sandwich composite deals with the maximum load-carrying capability and analyzing the damage under various conditions. Wang et al. [4] examined the quasi-static compressive response and observed that perforation size was the key parameter affecting the compressive attributes and deformation patterns. The

---

✉ Benedict Thomas
  benedict.thomas@vit.ac.in

[1] School of Mechanical Engineering, VIT, Vellore, Tamil Nadu 632014, India

crushing stress was more dependent on specimen dimensions than collapse stress. Upreti et al. [3] found that the maximum deformation was found at the central region and minimum at the fixed end. The stress distribution was discontinuous over the face sheet and maximum at the fixed supports. Wu et al. [1] used Nomex composite to perform three-point bending test which gave the ultimate load and the deflection in the structure. Under static loads, the same approach was used to estimate the failure analysis and was verified using FEM technique which gave similar results. Wang et al. [5] recorded the mechanical response of TPMS sheets and found that overall failure first occurred in the central region and then all around.

Fatigue tests recently got more attention to examine the life of specimens as well as the failure modes. Lohote and Kelkar [6] carried out fatigue analysis to investigate the specimen's life. The objective was to find the minimum number of cycles a structure can sustain at a particular load and Palomba et al. [7] concluded that bending behavior was independent of strain rate and reducing the support span decreases its fatigue life. Hussain et al. [8, 9] analyzed the static and fatigue response using three-point bending tests. The fatigue life declines with a rise in loading level. They concluded that the sandwich structure failed in various ways such as yielding of face, compression of the face sheet, core shear failure, and core delamination along the face sheet interface. Ma et al. [10] investigated fatigue response and concluded that the failure in the sandwich panel was because of the failure in the honeycomb core. Solmaz and Topkaya [11] investigated the flexural fatigue response using low-velocity impact and noted that core height was the parameter for the increased fatigue strength. Before impact loading, increase in core height increases the damage load, and damage was among core and face sheets. Wang et al. [12, 13] used conventional sheets and ceramic tile face sheet and performed three-point tests. In ceramic tiles, heavy buckling was observed in the core and cracks in the middle. Failure occurred at the mid-span but deformation was less at the front conventional sheet. With increased height, the load-carrying capability was found to be highest. Li et al. [14] tested the hierarchical hexagon core with different cell size and commented about the size having the best load-carrying capability. Bending strength was found to be improved in the conventional cores and stiffness was 1.4–1.8 times. Belan et al. [15] performed fatigue test on Titanium Ti-6Al-4V alloy and concluded that the three-point bending load was more suitable than using pull–push loads. The fatigue cracks were less at lower amplitudes and higher at the larger amplitudes. Maharjan et al. [16] observed that LSP was able to produce surface alterations and improved fatigue performance. Severe plastic deformation near the surface was produced which resulted in microstructure refinement and

inducing residual stresses. Experiments and simulations using three-point bending test were performed by Anandan et al. [17] under the effect of elevated temperatures. As the temperature increased to 100 °C, the strength got decreased by 9.2%, while the stiffness was unchanged. Lee et al. [18] studied failure modes, shear, and compression response. The compressive and shear strengths decreased when the temperature mounts to 300 °C.

Four-point bending tests were studied to analyze the toughness. with the loading rate. Belingardi et al. [19] observed the failure at compressed face and honeycomb cell walls in undamaged and damaged specimen, respectively. Abbadi et al. [20, 21] studied the fatigue behavior of aramid core and defects experimentally and concluded that L configuration was more substantial than W at the same load levels. Additionally, Yongqiang et al. [22–24] studied the vibration response of honeycomb sandwich under various methods. Wang et al. [25] performed free vibration analysis of sandwich panels and concluded that frequencies decrease with a rise in the density of the filling foam, and hence geometrical parameters have more influence.

Li et al. [26] achieved the specific energy absorption (SEA) in fractal-like honeycombs for various structures and found that the SEA can be incremented at least by 85%. With increase in cell numbers, it incremented at slow pace. Liu et al. [27] studied blast resistance performances having circular metallic tubes and compared the partial-filled and fully-filled circular core with the conventional model. Energy dissipation was better in the circular metallic core which concludes good advantage in blast resistance plate. Liu et al. [28] found out that SEA can broadly reflect the crashworthiness by developing the factors as plateau stress, densified strain, and relative density and the Poisson's ratio had a similar influence on SEA. Li et al. [29] predicted the sound absorption performance using a promising hierarchical acoustic metamaterial sound absorber. They demonstrated the crucial role of structural hierarchy in designing metamaterials having exceptional absorption properties. Yuan et al. [30] investigated the effect of projectile mass on damage behaviors of CFRP and observed smaller dimension projectiles caused localized and visible dent damage on the specimen for low energy impact while the larger ones with high energy impact showed delamination. The heavier mass had higher chances of producing larger bending deflection. Other factors included out-of-plane properties in hexagon honeycombs. Potluri and Rao [31] examined the value of elastic constants, it decreased with an increase in cell wall length. Low-velocity impact response on titanium honeycomb core was performed by Xie et al. [32]. The specimen initially experienced the linear elastic deformation followed by the crushing of the honeycomb core. Luo et al. [33] investigated sandwich panel with in-plane honeycombs with different Poisson's ratio and stated that Negative Poisson's ratio

results in higher load carrying capability while zero Poisson's ratio has a better energy absorption behavior.

Despite these, simulation work on ANSYS regarding the fatigue tests on the honeycomb sandwich is limited. Previous reported works have concluded that results obtained using FEM have shown good agreement with the results obtained from experiments. At present, fatigue failure is one of the elementary problems aerospace industries are dealing with. Ensuring that the integral model design is safe, fatigue strength is essential in the whole design process [1]. The work carried out so far has been performed experimentally and numerically, and the fatigue response has been validated from the available the literatures.

In the present work, the experiments were carried out under three-point bending conditions to investigate the static behavior and damage modes for the specimen using the combination of Al 3003 as core and *E*-Glass Fiber as face sheet. The results were validated using computational approach and further analysis on different material combinations was studied. The static and fatigue response for other material combinations with similar trend were investigated using the computational approach. The static deformation and equivalent stresses were observed to understand the flexural strength. The fatigue life of proposed model was discussed with the *S–N* diagrams.

2 Materials and methods

2.1 Material specification

The Honeycomb Sandwich composite was made by using several material combinations in the recent past. To validate the present computational work with the results available in the literature [9], Al 5052-H32 along with *E*-glass fiber as core and face sheets were used in the present work. Titanium and its alloys combined with different grades of Aluminium have recently capitalized themselves in every major field. In the present work, new materials were used, such as,

Al 6061-T6 which contains good corrosion resistance and weldability, Al 7075-T6 which provides good resistance to fatigue failure, high strength, toughness, and less dense, used as honeycomb core, and Ti-6Al-4V being titanium alloy applied as the face sheets offering high corrosion resistance and strength-to-weight ratio. The properties of these materials are listed in Table 1. The values were imported into the engineering library of ANSYS.

2.2 Modelling for honeycomb structure

The honeycomb model shown in Fig. 1 was modeled in SolidWorks. The dimensions of the Honeycomb core are $200 \times 28 \times 13.5$ mm. Face sheet with dimension $200 \times 28 \times 0.25$ mm is appended on both sides of the honeycomb core. The dimensions of the sandwich are mentioned in Table 2 [9].

2.3 Finite element analysis

The FEA was carried out in ANSYS (2019), a numerical study to solve engineering problems to the nearest approximations. The material properties were imported in the engineering library including the ultimate and fatigue stress limits and the *S–N* curve of the individual materials. In Design Modeler, the 3-point bending set-up was created as shown in Fig. 2. In static structural, the material selections were made for the core and face sheets. The coordinate system was embedded at the center of the specimen. During meshing, the body sizing was set to 3 mm for the honeycomb core and face sizing of 4 mm for the face sheets. The specimen was modeled using patch conforming algorithm under the tetrahedron method. The local fine mesh was generated as shown in Fig. 3.

2.3.1 Static three-point test

To investigate the static behavior, three-point bending tests need to be performed. It estimates the shear strength, shear

Table 1 Mechanical properties of core and face sheet

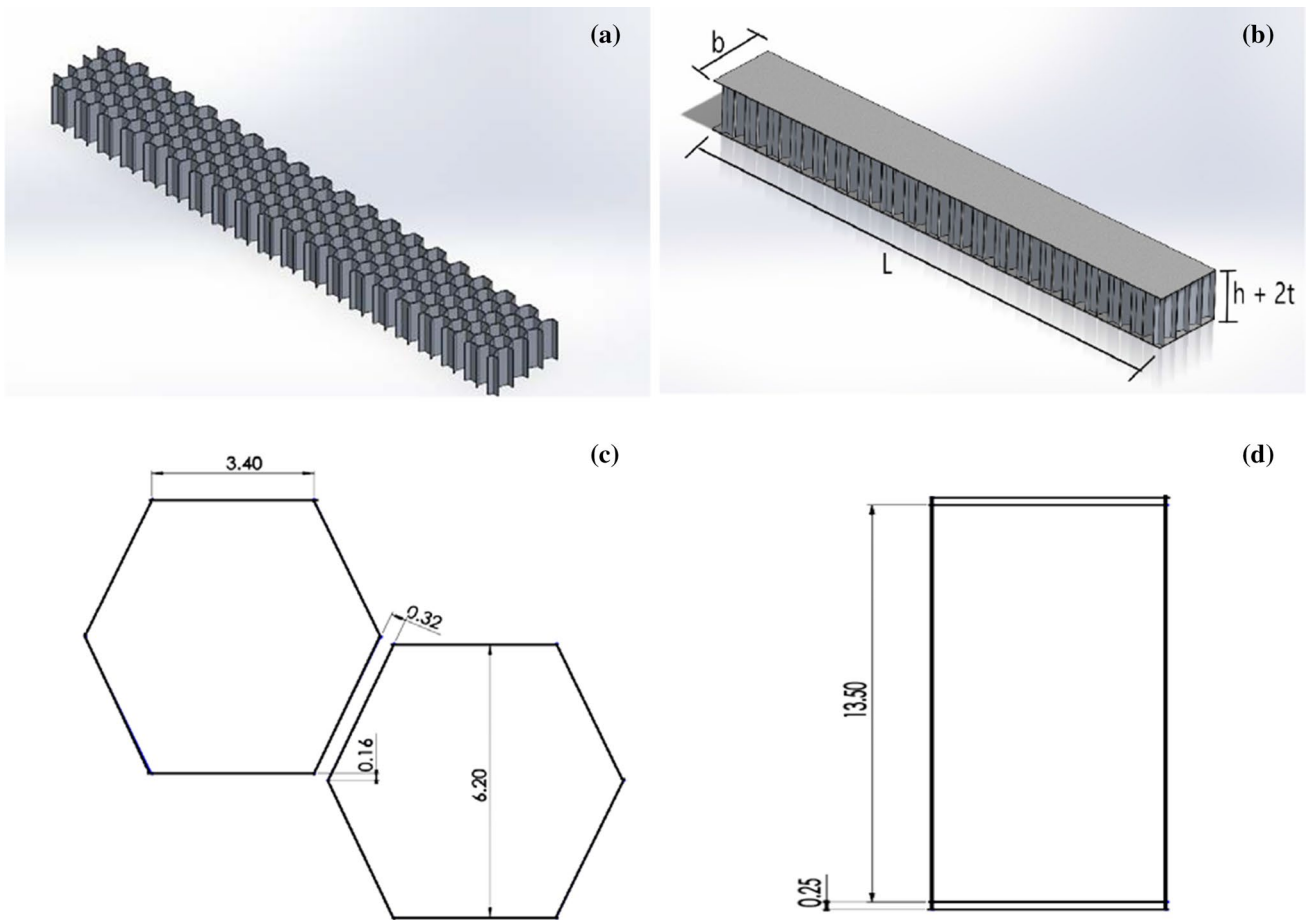| Properties	Al 6061-T6 core	Al 7075-T6 core	Ti-6Al-4V face sheet
Density (g/cc)	2.70	2.81	4.43
Poisson's ratio	0.33	0.33	0.32
Elongation at break (%)	17	9	10
Modulus of Elasticity (GPa)	68.90	71.70	107
Bulk modulus (GPa)	67.55	70.3	100.75
Tensile strength (MPa)	365	572	1300
Yield strength (MPa)	276	503	1180
Shear modulus (GPa)	25.90	26.96	40.43
Shear strength (MPa)	207	331	760

Fig. 1 Geometrical Representation of Honeycomb **a** Core **b** Sandwich Panel **c** Cell Wall **d** Height of panel

Table 2 Dimensions of honeycomb sandwich

Length L (mm)	Width b (mm)	Skin thickness t (mm)	Height of the core h (mm)	Thickness of core wall d (mm)	Length of cell edge l (mm)	Height of cell edge h_1 (mm)
200	28	0.25	13.5	0.32	3.4	6.2
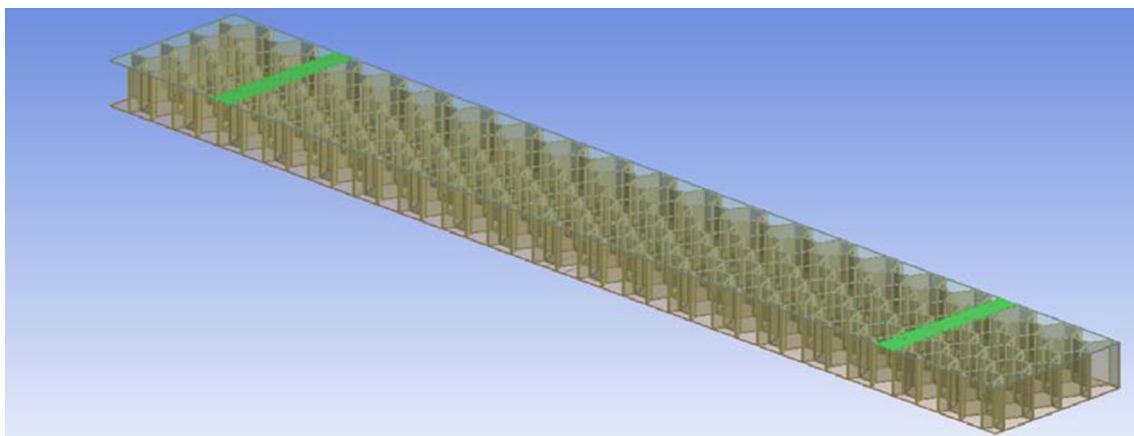
Fig. 2 Representation of three-point bending setup
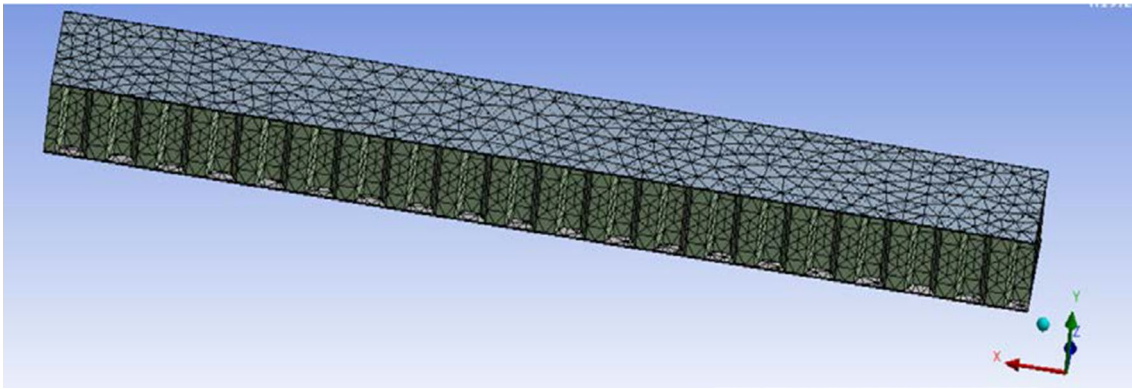
Fig. 3 Meshed model

elastic modulus, bending stiffness, and elasticity of the specimen. Figure 4 shows displacement and the applied load at the mid-region in y-direction. In solution, the total deformation and the equivalent Von-Mises stress were selected. The directional deformation is used to estimate the bending strength in a particular direction.

2.3.2 Fatigue three-point test

To investigate fatigue behavior, the value of ultimate and fatigue strength is prominent. The S–N curve of the materials used in the specimen is also crucial. The three-point bending analysis on the specimen is performed using the same boundary conditions as mentioned in static tests, shown in Fig. 4. Fatigue failure usually occurs in highly concentrated areas. In Solution, the fatigue tool is selected and stress value is set as Goodman, keeping the loading ratio as 0.1. The life of the specimen is estimated at various load values.

3 Fatigue life prediction

For computational analysis, S–N Curve for the material is crucial to analyze the behavior of the specimen. Basquin proposed a method to find the SN curve for below 10^6 cycles. The value of the alternating stress can be calculated using Eq. 1

$$\sigma_a = aN^b \tag{1}$$

where a and b are constants and can be found using the Eqs. 2 and 3. At $N = 10^4$, $\sigma_a = 0.95\sigma_u$ and at $N = 10^6$ cycles, $\sigma_a = \sigma_e$.

$$b = \frac{\log \sigma_e - \log \left(0.95\sigma_u\right)}{2} \tag{2}$$
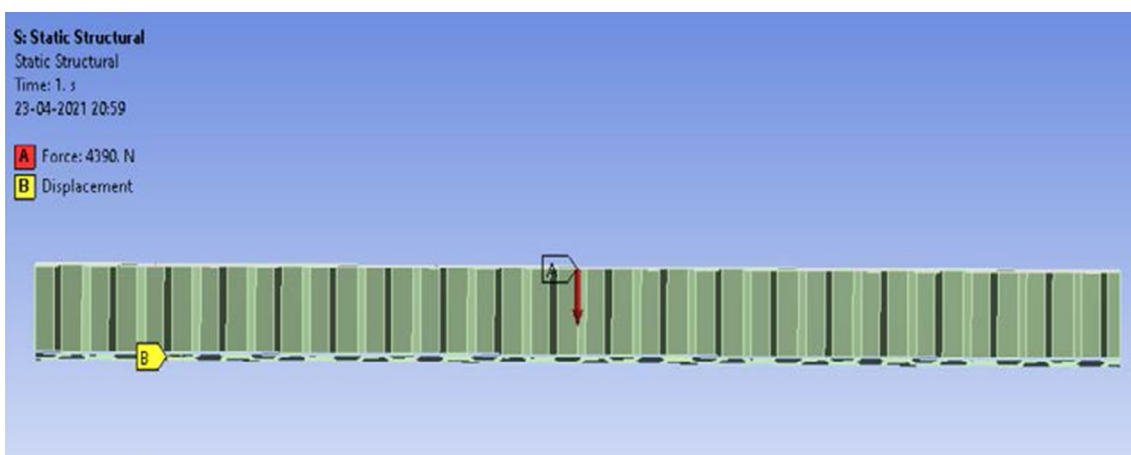
$$a = \frac{\sigma_e}{10^{6b}} \tag{3}$$

Fig. 4 Boundary conditions at maximum load

The goodman relation in Eq. 4 is used to relate σ_m, σ_a, σ_u, and σ_e.

$$\frac{\sigma_a}{\sigma_e} + \frac{\sigma_m}{\sigma_u} = 1 \tag{4}$$

The following relationship is required to correlate the fatigue and ultimate stress limits.

4 Results and discussion

After modeling, finite element analysis was carried out in order to discretize the structure. Further static and fatigue analysis of the structure has been performed and the obtained results were presented and discussed. To validate the simulation results, experimental test was performed on the honeycomb composite with Al 3003 as core and *E*-Glass Fiber as face sheets.

4.1 Static test results

The proposed structure is first analyzed for different static loads using 3-point bending set-up.

4.1.1 Experimental validation

To validate the computational static behavior results, experiments were carried out on the specimen Al 3003 and *E*-glass fiber. The honeycomb sandwich structure selected for this study is made of three materials. Glass fiber is used for face sheet while epoxy resin was used as a matrix. The hexagonal honeycomb used in specimens is made of aluminum Al 3003. The panel of sandwich structures prepared from vacuum bag molding technique was cut into the desired dimensions specimens. Two different specimens were tested with different dimensions $100 \times 50 \times 12$ mm (Specimen1) and $200 \times 30 \times 12$ mm (Specimen2), the thickness of core kept as 10 mm and face sheet as 1 mm. The size of cell was taken 6.35 mm and thickness of cell wall was 0.06 mm. The dimensions and geometry of honeycomb sandwich structures was given in Figs. 5 and 6.

According to standard ASTM C393, the three-point bending test was performed. The experimentation for the investigation of the bending strength and damage modes was carried out on INSTRON-8801 using three-point bending load configurations. The load is applied at the mid-span and deflection was recorded till the failure of the specimen. The final test data and damage modes are recorded. For each specimen, the testing was performed for two samples in order to achieve the maximum accuracy in the results as shown in Fig. 7. Both the specimens demonstrated various phases of deformation under the
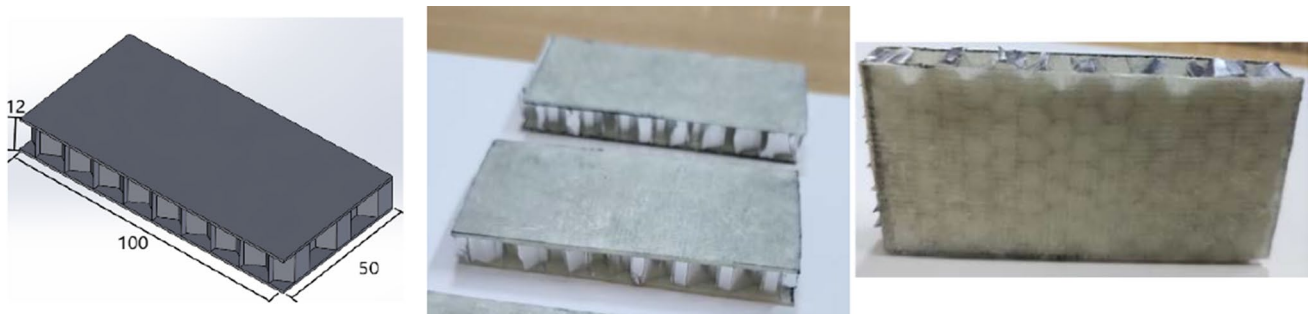

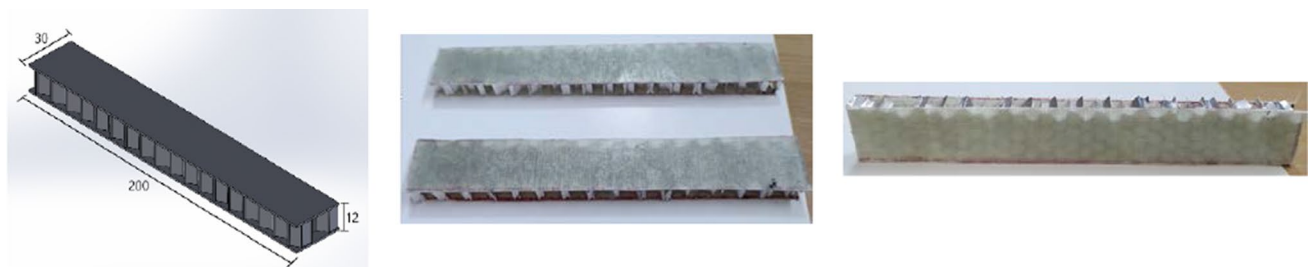**Fig. 5** Dimensions and geometry of honeycomb sandwich Specimen1

Fig. 6 Dimensions and geometry of honeycomb sandwich Specimen2
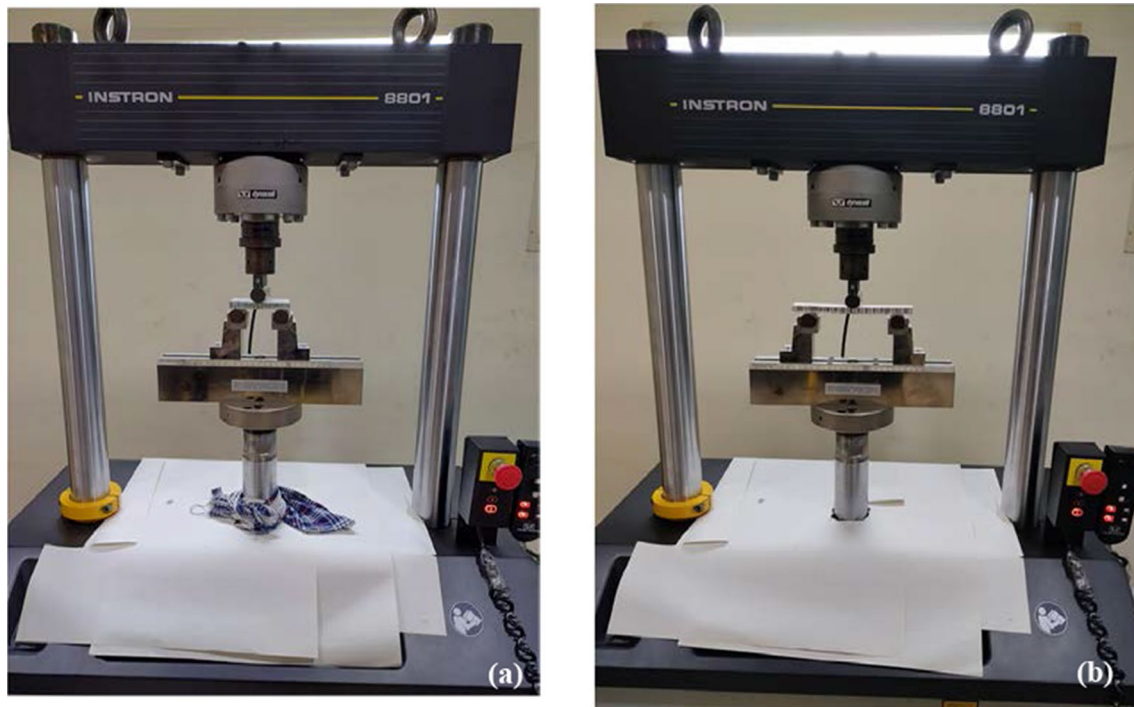
Fig. 7 Experimental setup and three-point loading arrangement for **a** Specimen1 **b** Specimen2

application of continuous load as shown in Figs. 8 and 9. Face yielding and compression of the face sheets were witnessed. It occurred due to the stress in the face sheet exceeding the material's elastic limit. Further loading on the specimen resulted in the interlaminar shear failure of facing and bending of cell wall.

Figures 10 and 11 describe load with displacement for both the specimens and the results were noted in the form of phases. An approximate linear relation between load and displacement is observed as shown in phase 1. Further increase in force causes little displacement which causes face yielding as shown in phase 2. The highest load value is achieved
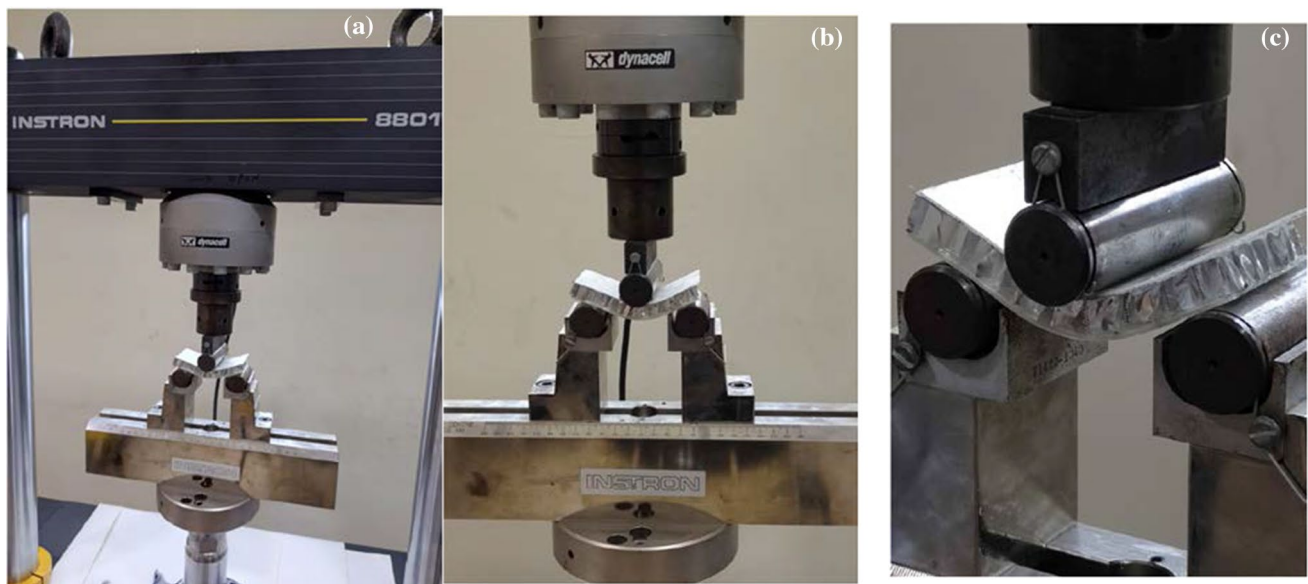
Fig. 8 Phases under static tests of Specimen1 **a** Under load **b** Face yielding and compression of face sheets **c** Interlaminar shear failure of facing and bending of cell wall
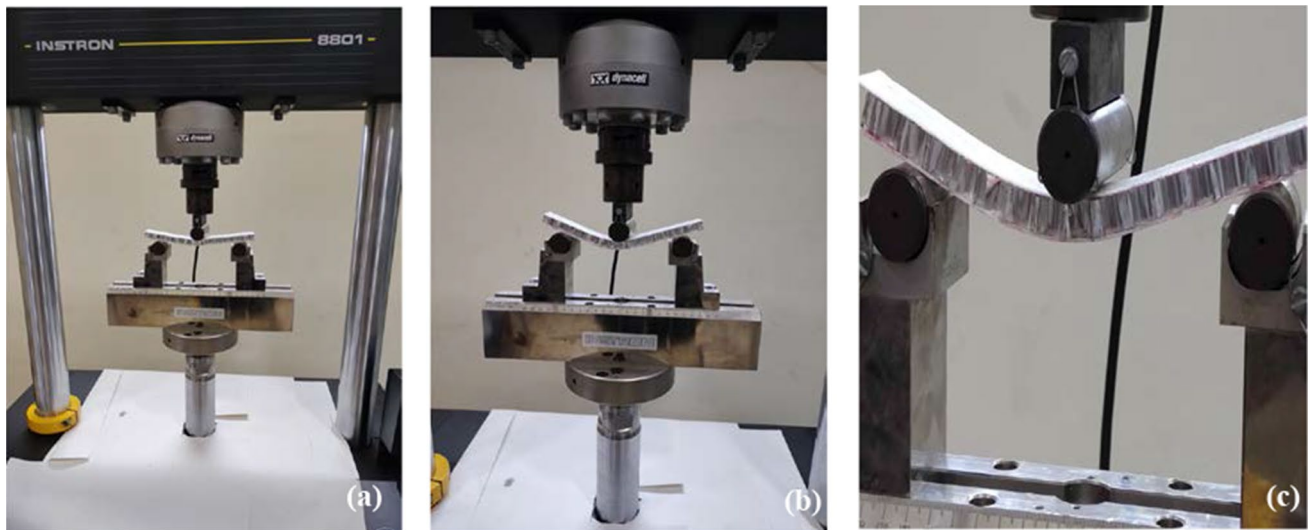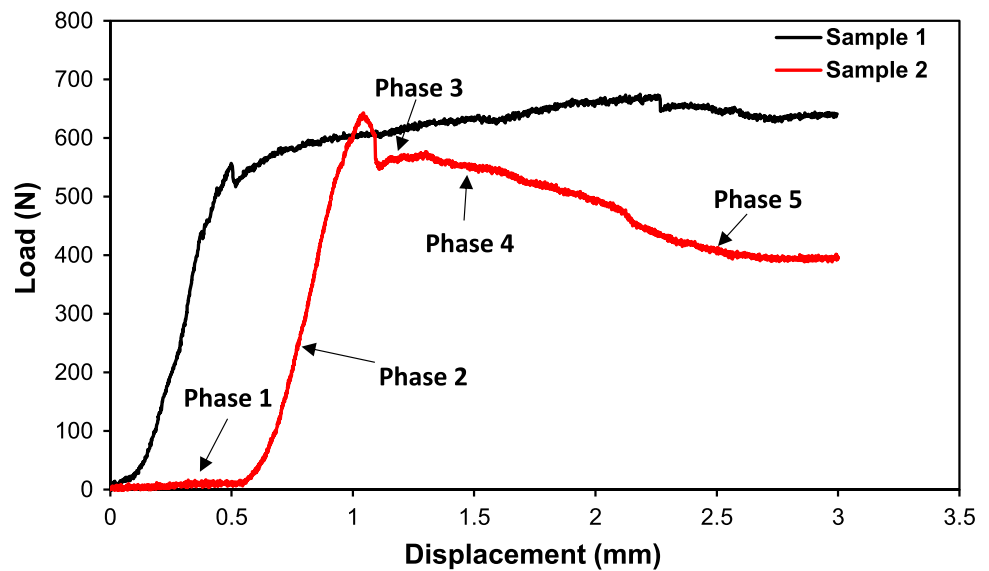
Fig. 9 Phases under static tests of Specimen2 **a** Under load **b** Face yielding and compression of face sheets **c** Interlaminar shear failure of facing and bending of cell wall

Fig. 10 Variation of load with displacement of Specimen1

at this point. An abrupt drop in load-carrying ability of the specimen was observed due to the indent shown in phase 3. Further displacement in the specimen is achieved as the load value kept on decreasing as shown in phase 4. Phase 5 shows increase in displacement upon further application of load.

The FEA was performed on the modeled specimens with same dimensions. The material properties were added to the software to analyze the deformation of the specimen. The deformation for the Specimen1 at the highest load of 811 N in the experimental work was found to be 13.27 mm while in the simulation the value was 10.22 mm. Similarly, for the Specimen2 at the highest load of 224 N, the value in the experimental work was found to be 0.82 mm while in

the simulation it was 0.69 mm. The failure types observed in the work were the bending of face sheet and the core. The first failure was observed in the core crushing. Figures 12 and 13 plots the trend obtained for force with displacement. The plot shows the linearity between both the curves and the simulation results were in good agreement with the experimental results.

4.1.2 Theoretical results for maximum deflection

For simply supported load with the given span and constrained to three-point bends, the total deflection was presented by two values; the first was due to bending of

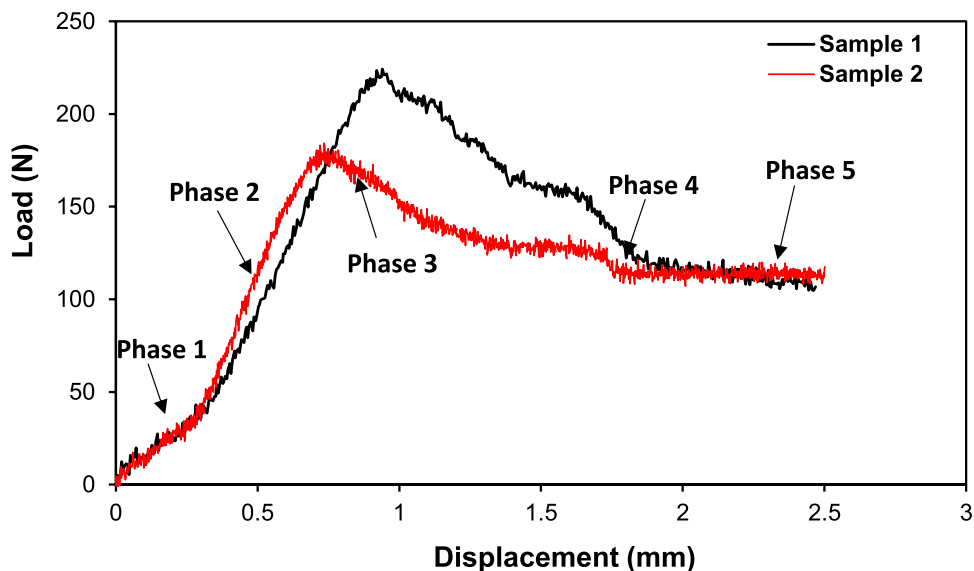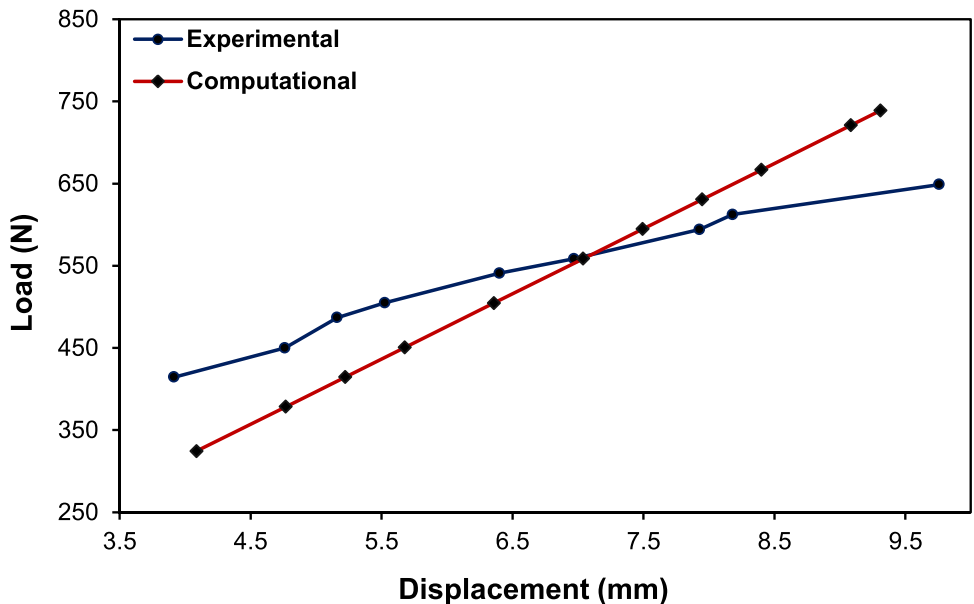**Fig. 11** Variation of load with displacement of Specimen2

Fig. 12 Comparison of load with displacement of Specimen1

the whole structure, the second was due to the transverse shear. The superposition principle is applied to unite the two deformations, but it was observed that the value of transverse shear was negligible. Hence, the maximum deflection can be calculated using Eq. 5 [3].

$$\delta_{max} = \frac{qL^4}{384EI} \tag{5}$$

where q is the load per unit length, L is the length of specimen, E is the elasticity of the face sheet and I is the moment of inertia can be calculated using Eq. 6.

$$I = \frac{btH^2}{2} \tag{6}$$

where H is the distance between centers of face sheets. The bending stiffness can be achieved using the formula $D = EI$. The bending calculations were performed and mentioned in Table 3.

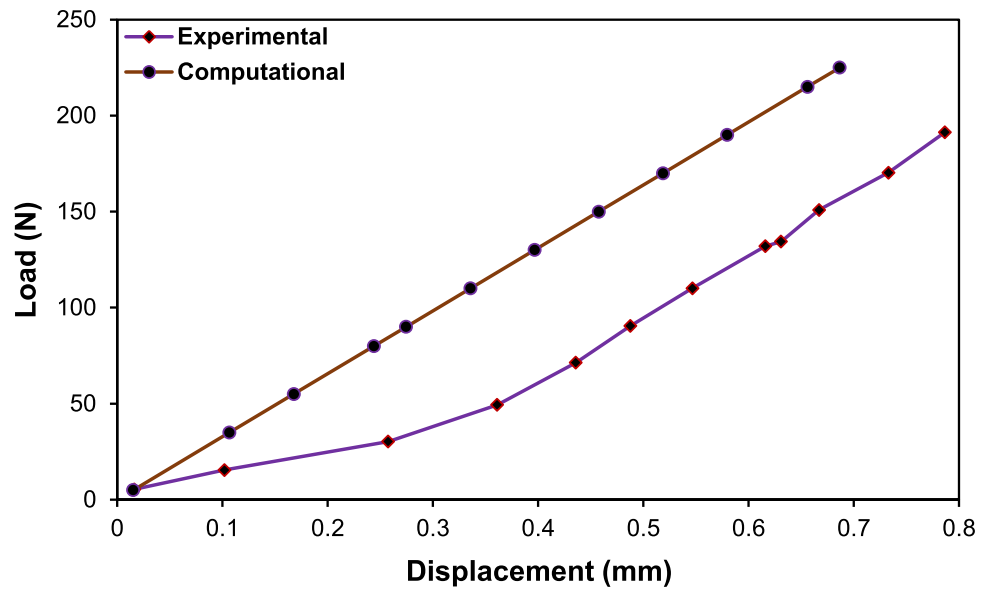**Fig. 13** Comparison of load with displacement of Specimen2

Table 3 Static test results for Al 7075-T6 and Ti-6Al-4V

| Load value (kN)	Deformation (mm)			Equivalent stress (MPa)		
	theoretical	Simulation	Error (%)	Maximum	Minimum	Average
4.170	2.0449	2.004	2.0	1112.1	0.0438	147.51
3.941	1.9376	1.8911	2.39	1117.2	0.0415	139.65
3.731	1.8297	1.7847	2.46	1102.7	0.0395	131.86
3.512	1.7223	1.6798	2.47	1040.9	0.0375	124.13
3.292	1.6144	1.5745	2.47	975.67	0.0352	116.36
3.073	1.5069	1.4698	2.46	910.77	0.0328	108.62
2.853	1.3991	1.3646	2.46	845.57	0.0305	100.84
2.634	1.2917	1.2598	2.47	780.67	0.0281	93.09
2.414	1.1838	1.1546	2.47	715.47	0.0258	85.32
2.195	1.0764	1.0499	2.46	650.56	0.0234	77.58
1.975	0.9685	0.9446	2.47	585.36	0.0211	69.81
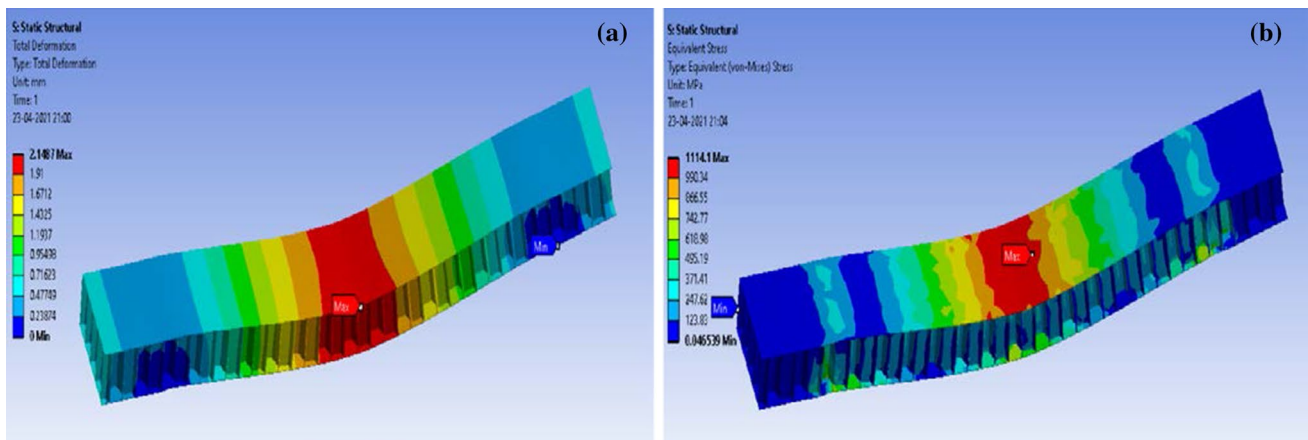
Fig. 14 Results at ultimate load **a** Deformation **b** Equivalent Stress

4.1.3 Simulation results

The load and displacement were applied to estimate the bending strength of the specimen. At several load levels (ratio of applied load and ultimate static load). Figure 14a describes the maximum deformation occurring at ultimate load, while Fig. 15 shows the deformation at various load values for Al 7075-T6 and Ti-6Al-4V. While the load was un-distributed all over the panel, it was evident that the maximum deformation occurred at the central region and lowest in areas where boundary conditions were given. The values were minimal that concludes its elastic nature.

The equivalent stress plays a vital role in the estimation of the fracture point. Figure 14b describes the maximum stress at ultimate load, while Fig. 16 gives the stress values at various loads for Al 7075-T6 and Ti-6Al-4V. Von-Mises stresses are used for the equivalent stress analysis; the average equivalent stress started decreasing as the load value decreases. The difference was observed uniformly throughout the loading levels for the specimen.

Figures 17 and 18 show the trend for deformation in various material combinations. The combination of Al 7075-T6 and Ti-6Al-4V, had lower deformation under the high load values. Table 3 shows the deformation values compared with the theoretical ones, and the results are similar. It confirms that the material composite has undergone very low deformation. The values symbolize that specimen has the ability to withstand high loads. The values were in the range of 1–2.2 mm for the applied loads. The values were examined with theoretical values, and results were comparable.

Figures 19 and 20 show the curve for the maximum equivalent stress against different load values. The maximum stress was observed in the material combination of Al 7075-T6 and Ti-6Al-4V. Table 3 shows the maximum and minimum values of the given series. It labels that the maximum stress was at the central region while the minimum stress was at the span of 120 mm. The maximum equivalent stress was in the range of 586–1121 MPa, while its minimum value was around 0.02 to 0.04 MPa. The values examined were within the span of the specimen.

To observe the overall bending in the specimen at the loads perpendicular to its length, normal stresses and strains should also be analyzed. The complete response under several loads can be seen in Figs. 21 and 22. The graphs reveal
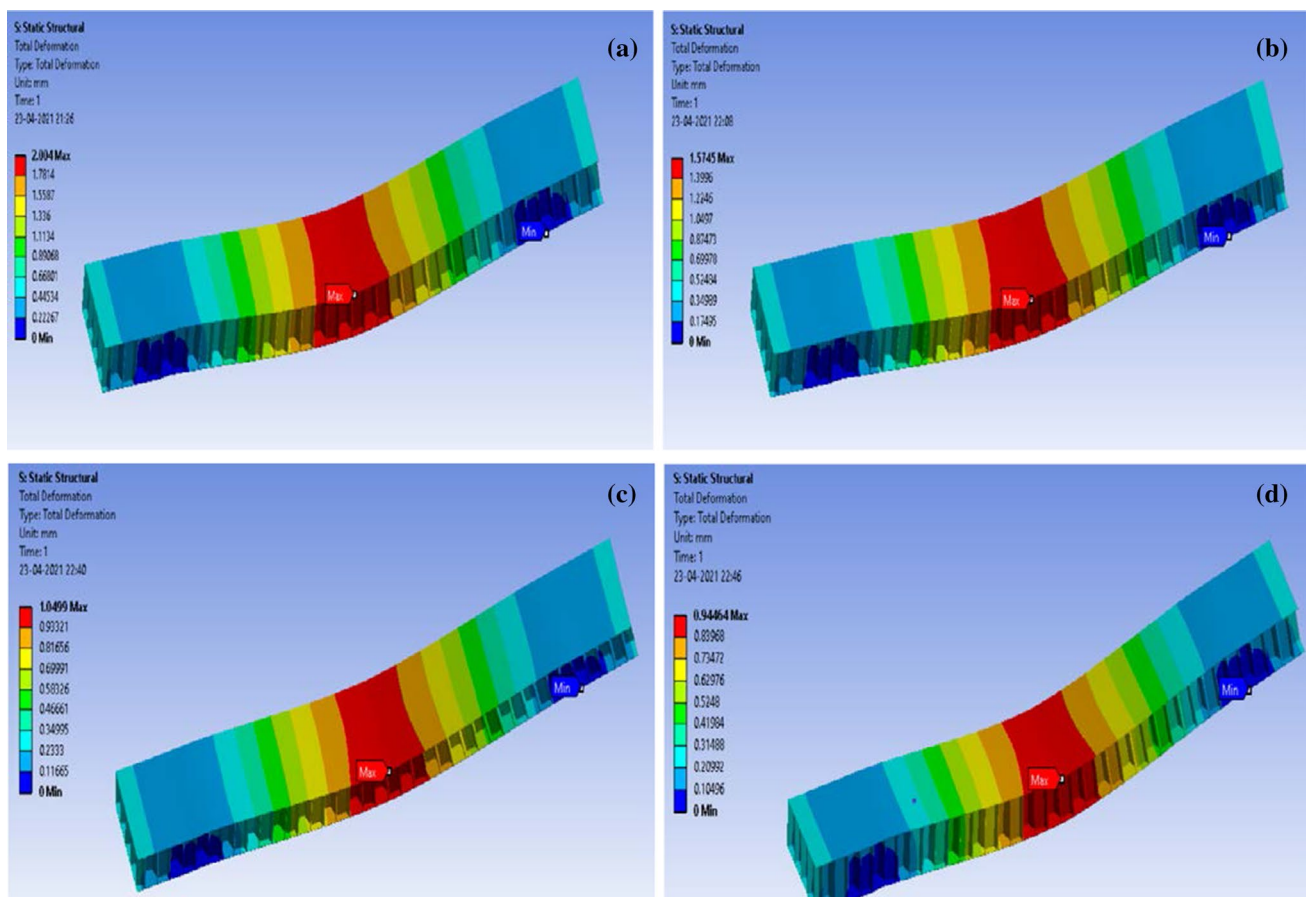

Fig. 15 Comparison of variation of load with deformation **a** 4.17 kN **b** 3.292 kN **c** 2.195 kN **d** 1.975 kN
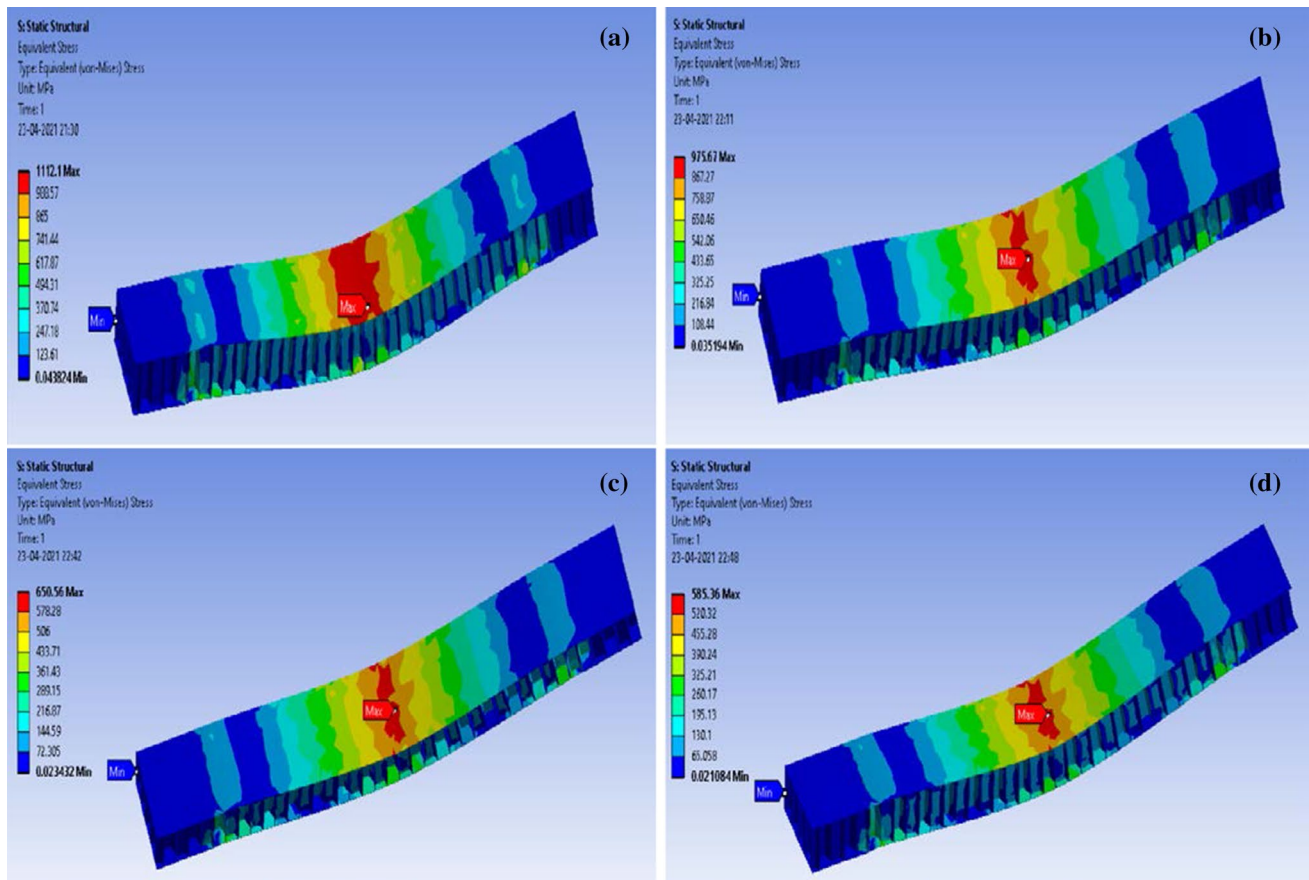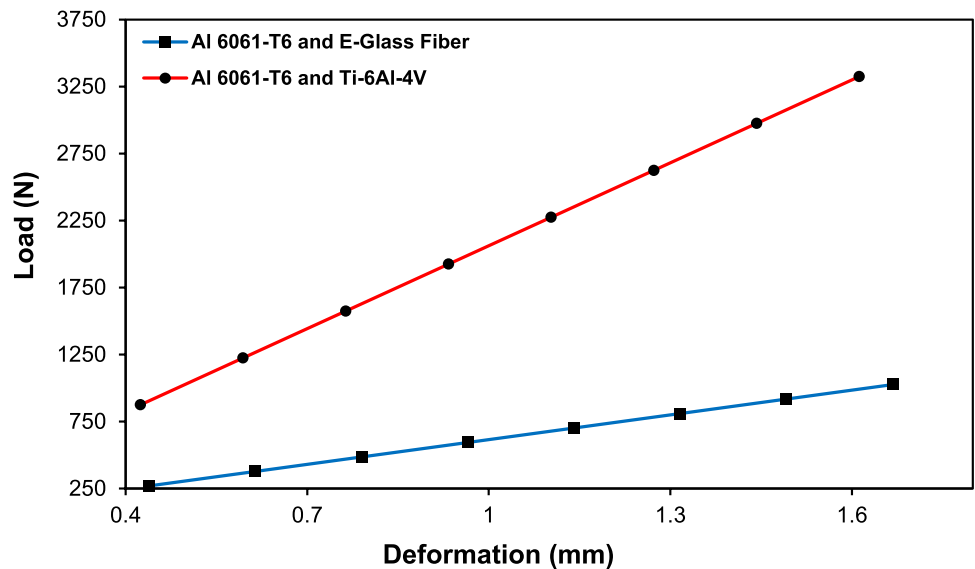
Fig. 16 Comparison of variation of load with Equivalent Stress **a** 4.17 kN **b** 3.292 kN **c** 2.195 kN **d** 1.975 kN

Fig. 17 Variation of load with deformation using Al 6061-T6 as core

that under continuous loading, the observed trend was linear. The strain values for the specimen were very low under bending loads. The results obtained for normal stress and strain at ultimate load were found to be 802.93 MPa and 0.0075, respectively. The uniformity was observed in the graphs which concludes the elastic behavior of the specimen. The maximum principal stress for the ultimate load occurred at the mid-span of the specimen and was found to

Fig. 18 Variation of load with deformation using Al 7075-T6 as core
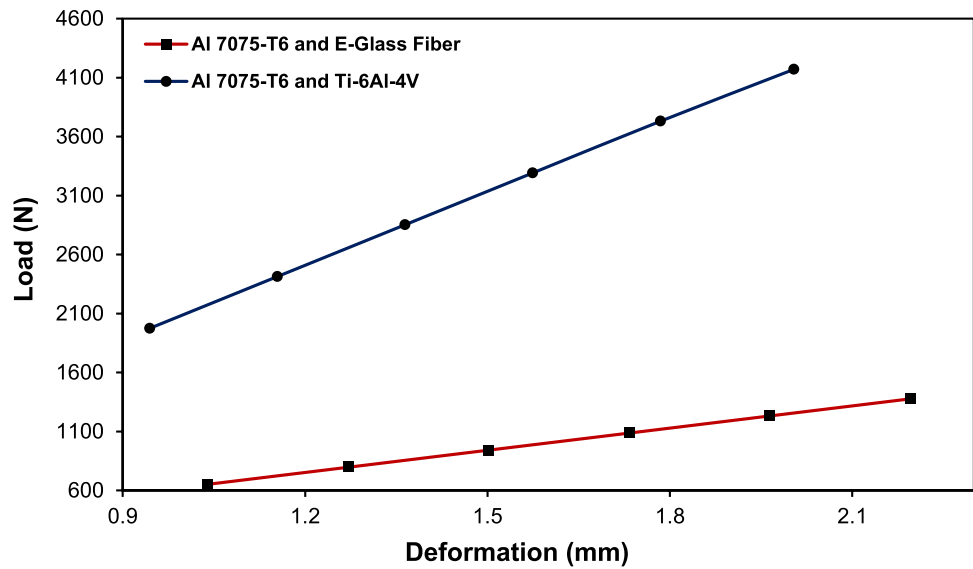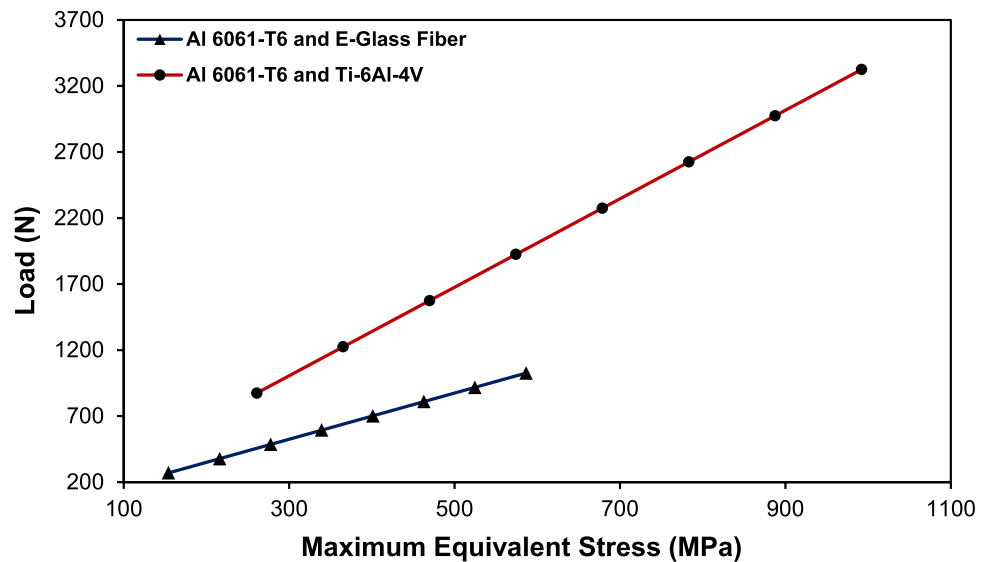

Fig. 19 Variation of load with equivalent stress using Al 6061-T6 as core

be 872.04 MPa while the minimum principal stress observed at the supports was found to be 166.23 MPa.

4.2 Fatigue test results

Fatigue analysis is carried out to investigate the life of the proposed structure under different loading conditions.

4.2.1 Fatigue life validation

Results in the present work are validated with the results available in the literature [9]. The same material combination was used for both core and face sheets. The properties have been imported into the engineering library. The same procedure was followed, and the simulated results for the fatigue life were compared. Table. 4 shows the validated results. The ultimate load was found to be around 950 N. The further work has been carried with proposed material combinations.

Figure 23 shows the variation of fatigue life at different load levels. It was evident that the results obtained from the computational analysis were similar. In both studies, it was observed that as the load value decreases, the minimum life increases approximately in a linear manner. It was concluded that the fatigue life reached an infinite number of cycles at 605 N.

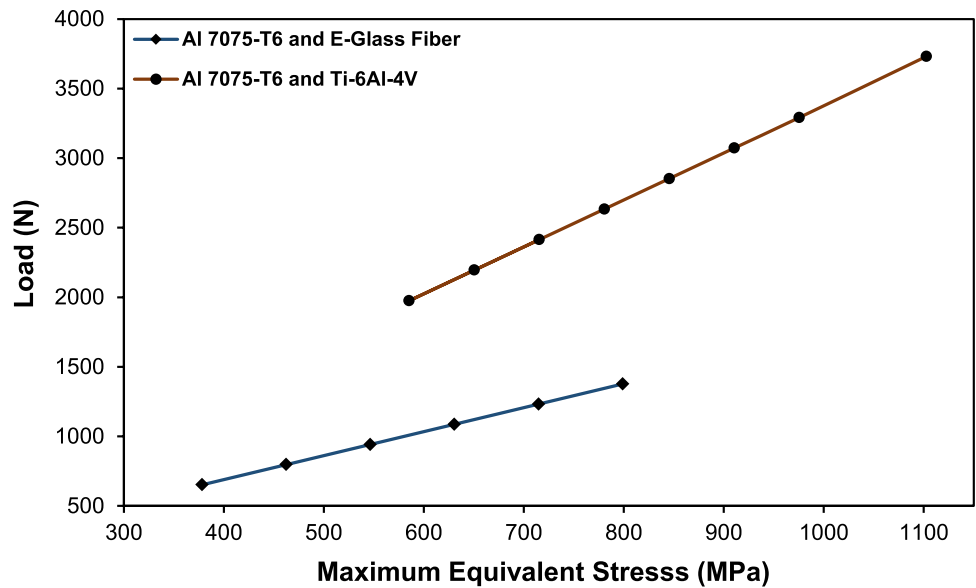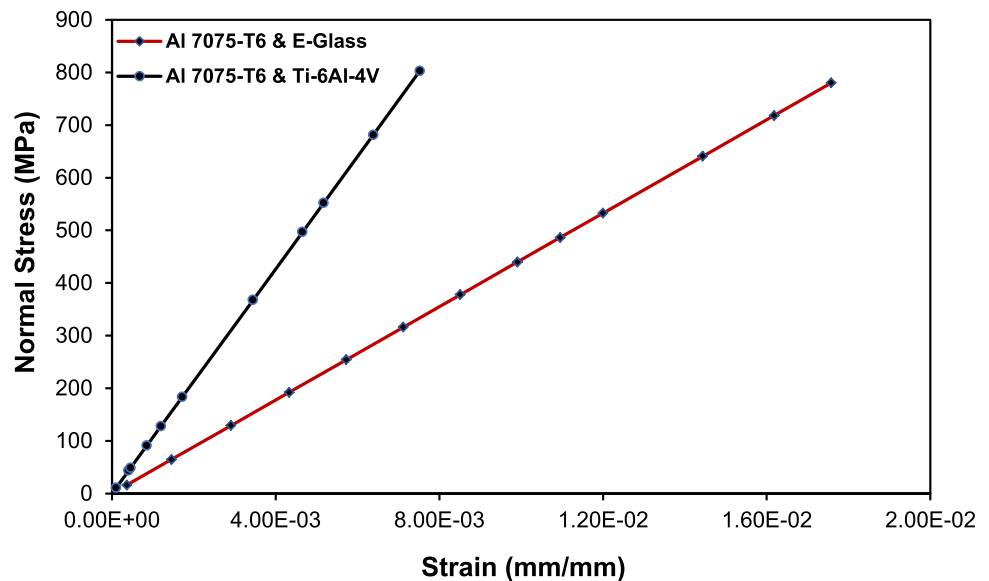**Fig. 20** Variation of load with equivalent stress using Al 7075-T6 as core

Fig. 21 Variation of normal stress with strain using Al 7075-T6 as core

4.2.2 Fatigue life

The fatigue test was conducted for the investigation of the minimum life. Before undergoing fatigue analysis, the *S–N* curve of individual material needs to be added accurately in the engineering library. The results for fatigue tests were achieved at different loads, and the graphs were plotted using the ultimate strength of the specimen. Several combinations were used to investigate the fatigue life, and it was observed that the combination of Al 7075-T6 and Ti-6Al-4V presented impressive results.

Before undergoing three-point bending tests, the shear loads were applied to the specimen to analyze shear failure of the core. Applying shear loads leads to the core shear. The results for the material combination of Al 7075-T6 and Ti-6Al-4V

was in good agreement and the specimen failed at the load of 3130 N. The shear stress and strain at this load were found to be 169.08 MPa and 0.0062 while the total deformation was recorded as 1.033 mm. While performing bending test, it was observed that the specimen had more capability to resist the loads. During simulation, the common modes of failure at high loads were the local indentation at the point of loading and the core shear. The maximum shear stress was found to be 586.08 MPa at failure load of 4390 N. At different loading levels, the fatigue life of the specimen was recorded. During the Fatigue analysis, the values followed a sharp trend to that of given load values. The maximum load-carrying capacity was determined when the fatigue life of the honeycomb sandwich composite was near zero. Figures 24 and 25 concludes that the failure at the higher loading level is due to the face

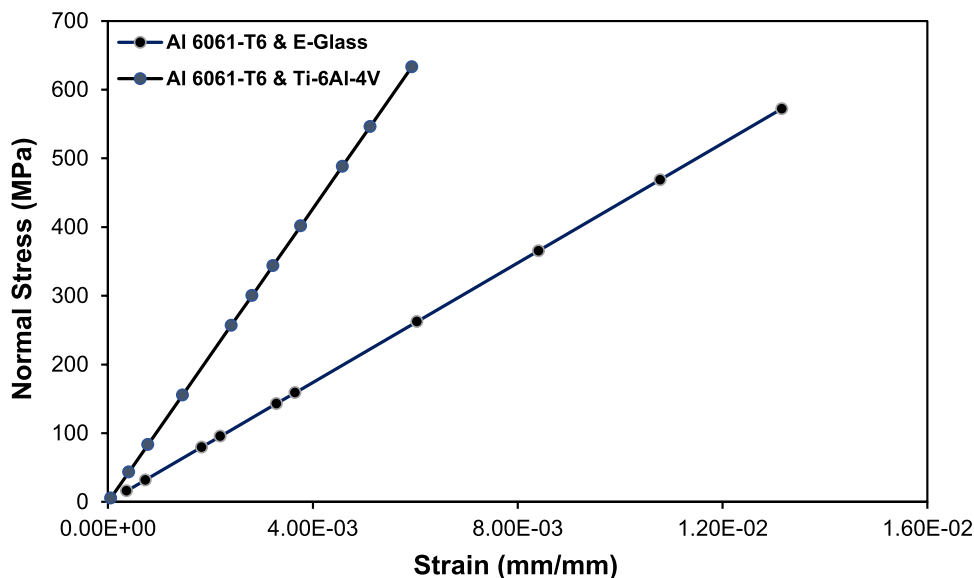**Fig. 22** Variation of normal stress with strain using Al 6061-T6 as core

**Table 4** Validation results for fatigue life

Load level	Load value (N)	Number of cycles Ref. [9]	Present
0.95	879	11,914	5579
0.9	833	27,291	20,244
0.85	787	78,155	55,204
0.8	740	142,440	124,140
0.75	694	207,200	294,960
0.7	648	580,200	671,160
0.65	601	1,000,000	1,000,000

sheet, while at the lower levels, the body fails due to the core and face sheet.

Table 5 shows the minimum life at different load values for the given series. It is evident from results presented in Table 5 that as the load value decreases, the minimum life of the specimen increases significantly. So, it is clear from the results that the proposed honeycomb structure shows enhancement in fatigue strength. The relationship between fatigue life and load level will be more significant in further studies. The equation suggesting the behavior for honeycomb composite can be expressed as shown below:

$$y = \left(5 \times 10^{10}\right)e^{-21.87x} \tag{7}$$
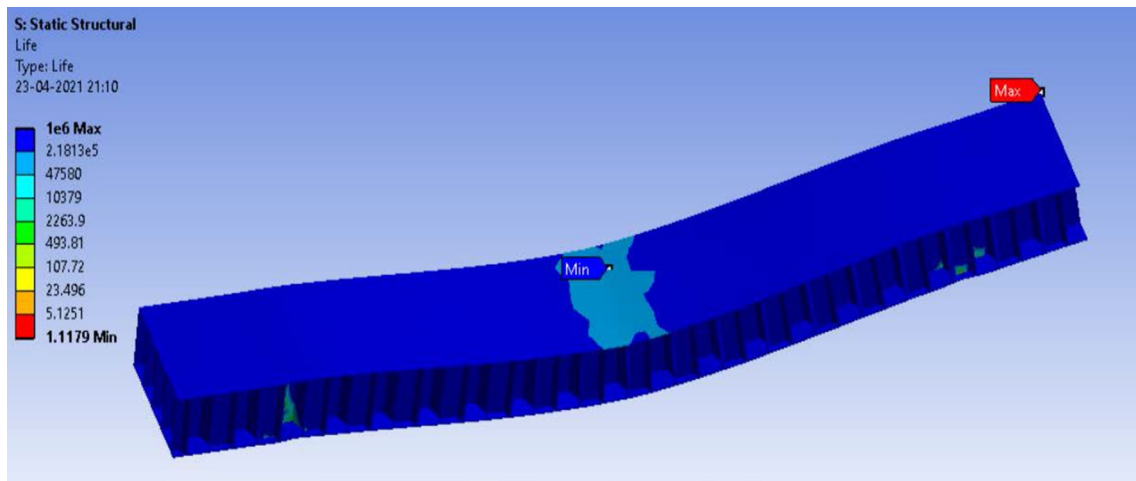
Fig. 23 Validation of fatigue life
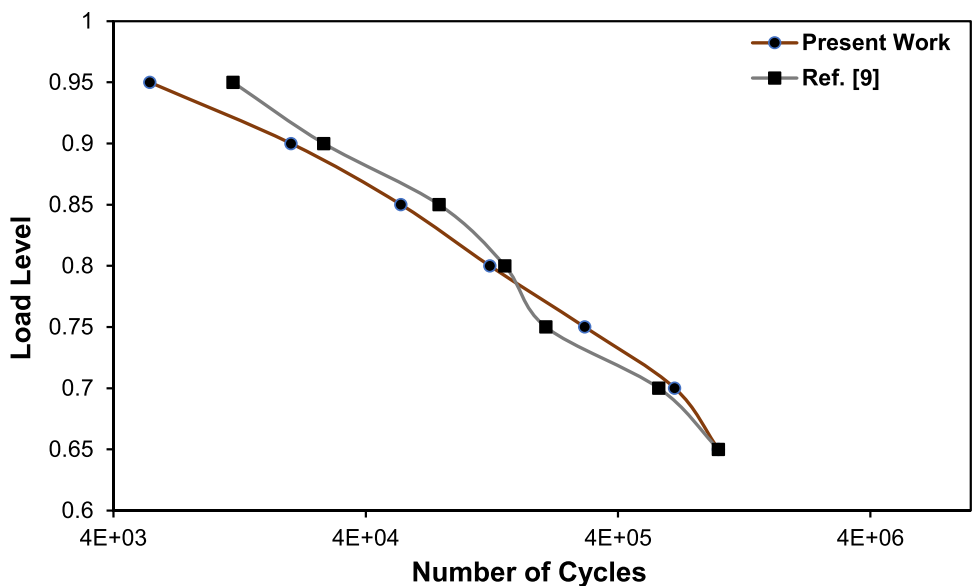
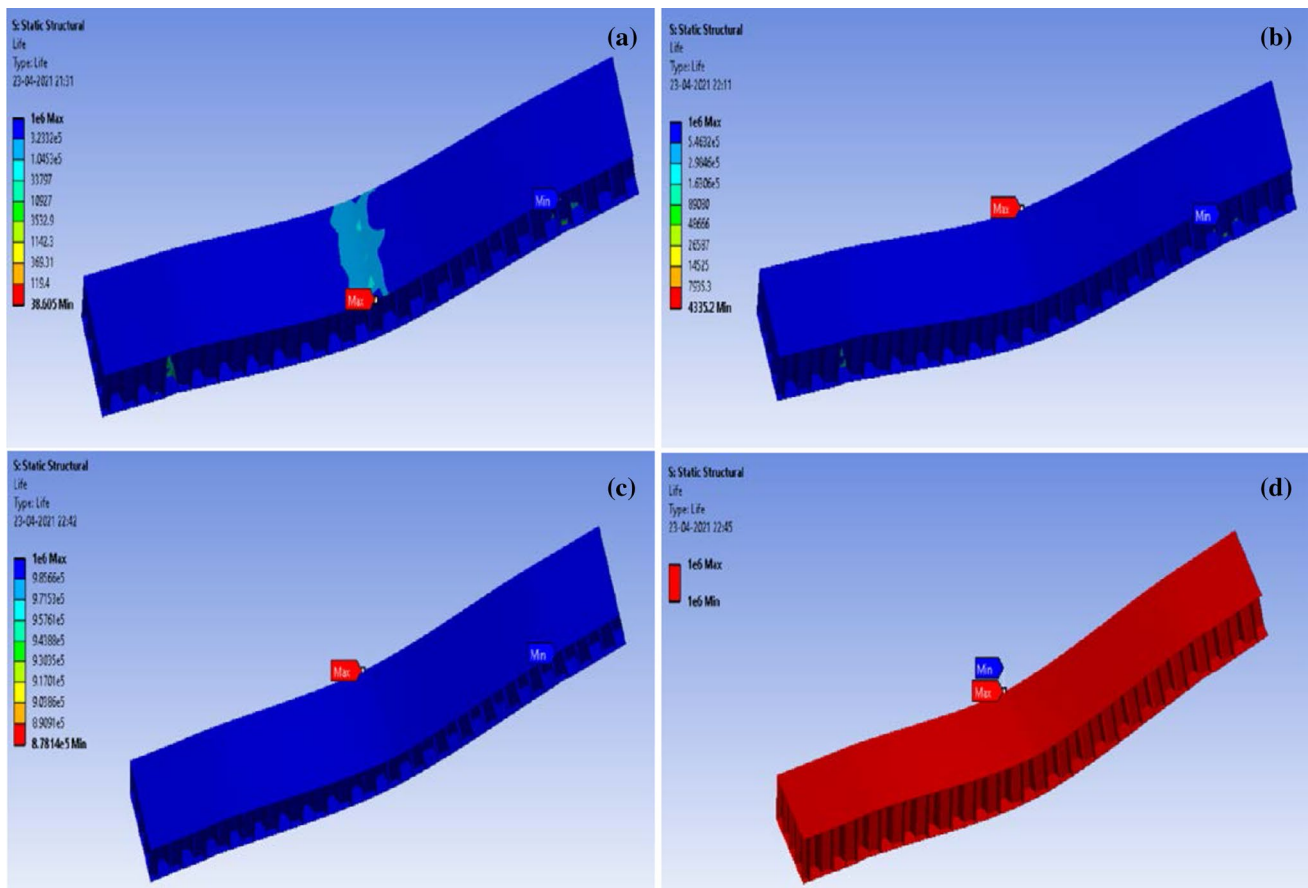**Fig. 24** Fatigue life of panel at 4.39 kN (Ultimate Load)

Fig. 25 Fatigue life of panel at **a** 4.17 kN **b** 3.292 kN **c** 2.195 kN **d** 1.975 kN

where y is the no. of cycles to failure and x is the load level corresponding to the load value.

Figures 26 and 27 display the trend of the *S–N* curve of the overall composite i.e., the minimum life with respect to load values. When the other materials were tested, the comparison was done, which can be witnessed in Fig. 28. At ultimate static load, the small face yields and delamination in the honeycomb core were observed, and cracks begin

Table 5 Fatigue test results of Al 7075-T6 and Ti-6Al-4V

Load level	Load value (kN)	Minimum life (number of cycles)
0.95	4.170	38.605
0.9	3.941	149.18
0.85	3.731	475.65
0.8	3.512	1,494.1
0.75	3.292	4,335.2
0.7	3.073	12,526
0.65	2.853	36,214
0.6	2.634	100,300
0.55	2.414	292,850
0.5	2.195	878,140
0.45	1.975	1,000,000

to propagate within the face sheet and core at the central region. It is because the load was applied at the mid-span of the specimen. Initially, the minimum life of the model starts to increase gradually, but as the load value decreases, it increases exponentially moving towards infinite cycles.

If loads are applied continuously, the specimen will be able to withstand the compression and bending. After this point, the load-carrying capability of the specimen decreases due to indentation within the span. The little stabilization is still present because of the shear resistance present in the core even after its failure. It infers that specimen fails due to the indentation at the located region. In static structural, the load is applied centrally to study the deformation. It was evident that the specimen failed because of the face sheet failure.

5 Conclusion

Static and fatigue behaviors were investigated for honeycomb sandwich composite under three-point bending conditions. Under static test, the deformation and equivalent stress were analyzed for different load values. Several material combinations were studied and it was observed that the combination of Al 7075-T6 and Ti-6Al-4V gave optimum results. At the highest load value of 4.4 kN, the overall deformation was determined to be 2.15 mm and the values were close to the theoretical results. The maximum and minimum equivalent stress were witnessed as 1114.1 MPa and 0.047 MPa, which proves the specimen's ability to resist high stress. Under fatigue test, the fatigue life of specimen was examined at several loads. Further, Experimental tests were also carried out to validate the computational analysis. The results were validated and displayed a good agreement with the results available in the literature. The proposed sandwich structure gave promising results. To analyze the shear failure in the specimen, shear loads were applied and the failure was observed at 3130 N. Under three-point test, the specimen showed capability to withstand high loads. The minimum value was scrutinized at 4.39 kN and it reached an infinite number of cycles around 2.1 kN. It infers that the specimen offers high shear and bending stiffness achieved. The present work intended to investigate different material combinations and parameters using computational technique
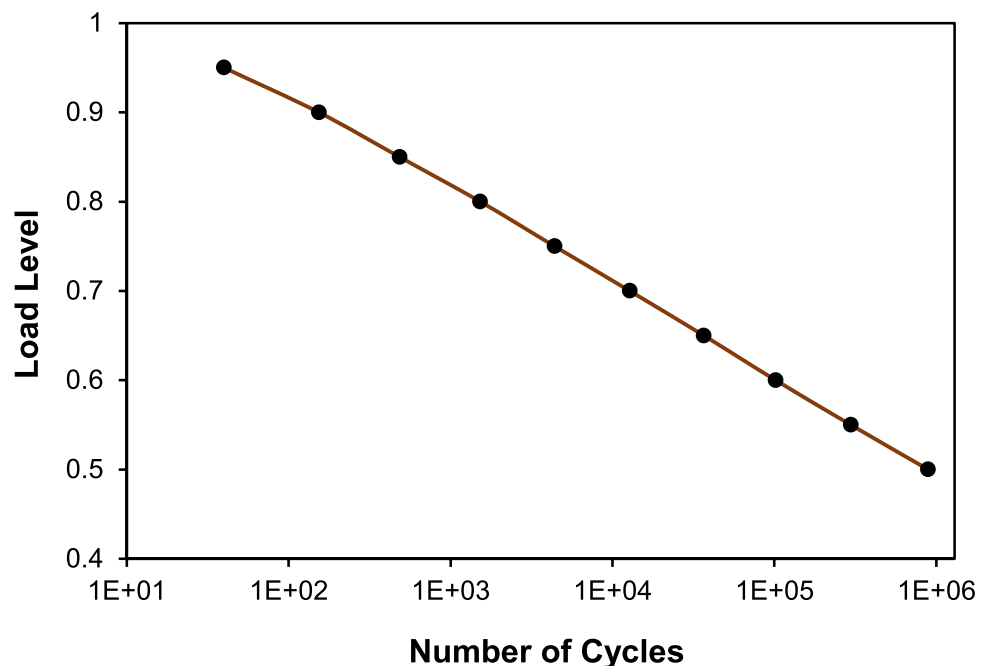
Fig. 26 Fatigue test results at different load levels

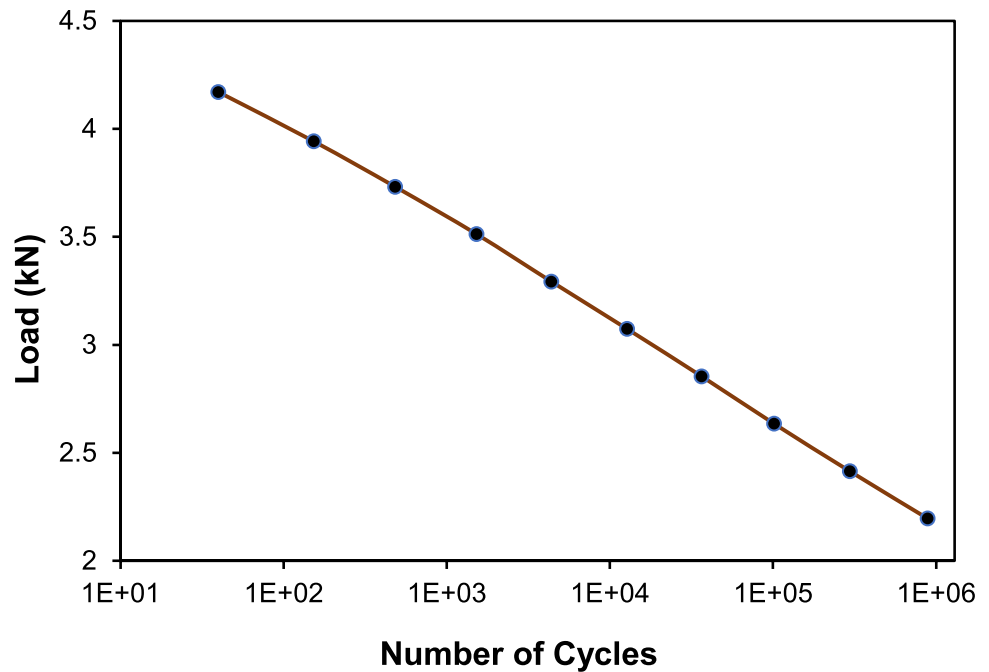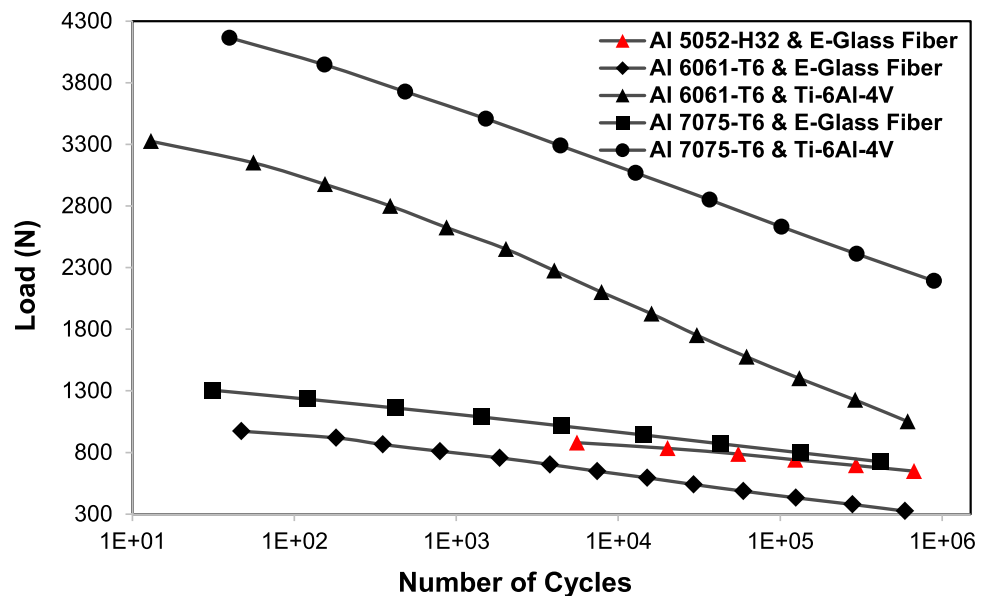**Fig. 27** Fatigue test results at different load values

Fig. 28 Fatigue test results with various material combinations

in order to achieve better static and fatigue characteristics. It has been accomplished by achieving maximum accuracy with the results. The proposed material combination is anticipated to be highly feasible in aerospace applications.

References

1. Wu X, Yu H, Guo L, Zhang L, Sun X, Chai Z (2019) Experimental and numerical investigation of static and fatigue behaviors of composites honeycomb sandwich structure. Compos Struct 213:165–172

2. Chemami A, Bey K, Gilgert J, Azari Z (2012) Behavior of composite sandwich foam-laminated glass/epoxy under solicitation static and fatigue. Compos Part B Eng 43(3):1178–1184

3. Upreti S, Singh VK, Kamal SK, Jain A, Dixit A (2020) Modelling and analysis of honeycomb sandwich structure using finite element method. Mater Today Proceed 25(4):620–625

4. Wang Z, Qin Q, Chen S, Yu X, Li H, Wang TJ (2017) Compressive crushing of novel aluminum hexagonal honeycombs with perforations: experimental and numerical investigations. Int J Solids Struct 126–127:187–195

5. Wang Z, Wang X, Gao T, Shi C (2020) Mechanical behavior and deformation mechanism of triply periodic minimal surface sheet under compressive loading. Mech Adv Mat Struct 28(19):2057–2069

6. Lohote A, Kelkar SS (2017) Fatigue analysis and life prediction of honeycomb structures. Int J Sci Adv Res Tech 3(2):46–50

7. Palomba G, Crupi V, Epasto G (2019) Collapse modes of aluminium honeycomb sandwich structures under fatigue bending loading. Thin-Walled Struct 145:106363

8. Hussain M, Khan RU, Badshah S, Abbas Z, Ijaz M, Khan S (2017) Investigation of static and fatigue behavior of honeycomb sandwich structures under bending load. Univ Eng Technol (UET) Taxila Tech J 22:72–80

9. Hussain M, Khan R, Abbas N (2019) Experimental and computational studies on honeycomb sandwich structures under static and fatigue bending load. J King Saud Univ Sci 31(2):222–229

10. Ma M, Yao W, Jiang W, Jin W, Chen Y, Li P (2020) Fatigue behavior of composite sandwich panels under three point bending load. Poly Test 91:106795

11. Solmaz MY, Topkaya T (2020) The flexural fatigue behavior of honeycomb sandwich composites following low velocity impacts. Appl Sci 10(20):7762

12. Wang Z, Li Z, Xiong W (2018) Experimental investigation on bending behavior of honeycomb sandwich panel with ceramic tile face-sheet. Compos Part B Eng 164:280–286

13. Wang Z, Li Z, Xiong W (2019) Numerical study on three-point bending behavior of honeycomb sandwich with ceramic tile. Compos Part B Eng 167:63–70

14. Li Z, Wang Z, Wang X, Zhou W (2020) Bending behavior of sandwich beam with tailored hierarchical honeycomb cores. Thin-Walled Struct 157:107001

15. Belan J, Kucharikova L, Tillova E, Chalupova M (2019) Three-point bending fatigue test of Ti6Al4V Titanium alloy at room temperature. Adv Mater Sci Eng 2842416:1–11

16. Maharjan N, Chan SY, Ramesh T, Nai PG, Ardi DT (2020) Fatigue Performance of laser shock peened Ti6Al4V and Al6061-T6 alloys. Fatigue Fract Eng Mater Struct 44(3):733–747

17. Anandan S, Dhaliwal G, Ganguly S, Chandrashekhara K (2018) Investigation of sandwich composite failure under three-point bending: simulation and experimental validation. J Sand Struct Mater 22(6):1–21

18. Lee HS, Hong SH, Lee JR, Kim YK (2002) Mechanical behavior and failure process during compressive and shear deformation of honeycomb composite at elevated temperatures. J Mater Sci 37(6):1265–1272

19. Belingardi G, Martella P, Peroni L (2007) Fatigue analysis of honeycomb-composite sandwich beams. Compos Part A Appl Sci Manuf 38(4):1183–1191

20. Abbadi A, Azari Z, Belouettar S, Gilgert J, Freres P (2010) Modelling the fatigue behaviour of composites honeycomb materials (aluminium/aramide fibre core) using four-point bending tests. Int J Fatigue 32(11):1739–1747

21. Abbadi A, Tixier C, Gilgert J, Azari Z (2015) Experimental study on the fatigue behaviour of honeycomb sandwich panels with artificial defects. Compos Struct 120:394–405

22. Yongqiang L, Dawei Z (2009) Free flexural vibration analysis of symmetric rectangular honeycomb panels using the improved Reddy's third-order plate theory. Compos Struct 88(1):33–39

23. Yongqiang L, Feng L, Dawei Z (2010) Geometrically nonlinear free vibrations of the symmetric rectangular honeycomb sandwich panels with simply supported boundaries. Compos Struct 92(5):1110–1119

24. Yongqiang L, Dawei Z (2011) Geometrically nonlinear forced vibrations of the symmetric honeycomb sandwich panels affected by the water. Compos Struct 93(2):880–888

25. Wang Y, Zhang Z, Xue X, Zhang L (2019) Free vibration analysis of composite sandwich panels with hierarchical honeycomb sandwich core. Thin-Walled Struct 145:106425

26. Li Z, Shen L, Wei K, Wang Z (2021) Compressive behaviors of fractal-like honeycombs with different array configurations under low velocity impact loading. Thin Walled Struct 163:107759

27. Liu J, Wang Z, Hui D (2018) Blast Resistance and parametric study of sandwich structure consisting of honeycomb core filled with circular metallic tubes. Compos Part B Eng 145:261–269

28. Liu J, Chen W, Hao H, Wang Z (2021) In-plane crushing behaviors of hexagonal honeycombs with different Poisson's ratio induced by topological diversity. Thin-Walled Struct 159:107223

29. Li Z, Wang Z, Guo Z, Wang X, Liang X (2021) Ultra-broadband sound absorption of a hierarchical acoustic metamaterial at high temperatures. Appl Phys Lett 118:161903

30. Yuan K, Liu K, Wang Z, Wei K, Yang M (2021) Dynamic fracture in CFRP laminates: Effect of projectile mass and dimension. Eng Fract Mechan 251:107764

31. Potluri R, Koteswara RU (2017) Determination of elastic properties of reverted hexagonal honeycomb core: FEM approach. Mater Today Proceed 4(8):8645–8653

32. Xie Z, Zhao W, Wang X, Hang J, Yue X, Zhou X (2017) Low-velocity impact behaviour of titanium honeycomb sandwich structures. J Sand Struct Mater 20(8):1–19

33. Luo Y, Yuan K, Shen L, Liu J (2021) Sandwich panel with in-plane honeycombs in different Poisson's ratio under low to medium impact loads. Rev Adv Mater Sci 60(1):145–157